



Wood identification based on longitudinal section images by using deep learning

Fanyou Wu¹ · Rado Gazo¹ · Eva Haviarova¹ · Bedrich Benes²

Received: 5 August 2020 / Accepted: 23 January 2021

© The Author(s), under exclusive licence to Springer-Verlag GmbH, DE part of Springer Nature 2021

Abstract

Automatic species identification has the potential to improve the efficacy and automation of wood processing systems significantly. Recent advances in deep learning allowed for the automation of many previously difficult tasks, and in this paper, we investigate the feasibility of using deep convolutional neural networks (CNNs) for hardwood lumber identification. In particular, two highly effective CNNs (ResNet-50 and DenseNet-121) as well as lightweight MobileNet-V2 were tested. Overall, 98.2% accuracy was achieved for 11 common hardwood species classification tasks.

Introduction

Current lumber scanners, used in industrial wood manufacturing plants, such as rough mills and flooring plants, are used to measure and evaluate the quality and optimize processing of solid wood (Gazo et al. 2018; Wells et al. 2018). Because wood species differ significantly in their color, grain structure, natural characteristics, defects, and density, the scanner sensors often need to be calibrated for each species for their optimal performance. When production switches from one species to another one, the scanner settings must often be manually set. In this

✉ Bedrich Benes
bbenes@purdue.edu

Fanyou Wu
wu1297@purdue.edu

Rado Gazo
gazo@purdue.edu

Eva Haviarova
ehaviar@purdue.edu

¹ Department of Forestry and Natural Resources, Purdue University, West Lafayette, IN 47906, USA

² Department of Computer Graphics Technology and Computer Science, Purdue University, West Lafayette, IN 47906, USA

study, we attempt to automate the species identification based on image recognition so that the manufacturing equipment can automatically adapt to species being processed or even be able to process batches of mixed species.

Convolutional neural network (CNN) is a deep learning architecture inspired by the natural visual perception mechanism of the living creatures. Lecun et al. (1998) developed a multi-layer neural network called LeNet-5, which could classify handwritten digits from the MNIST data-set. Recent CNNs are comprised of groups of convolutional, pooling, activation, and fully-connected linear functions, and they include hundreds of thousands of connections (Goodfellow et al. 2016). Batch Normalization (BN) and Dropout layers are often applied in the training phase. BN can speed up the training, while Dropout is a regularization tool that can mitigate overfitting (Ioffe and Szegedy 2015; Srivastava et al. 2014). There are many CNN architectures. Among them ResNet, DenseNet, and MobileNet-V2 are commonly used (Huang et al. 2017; He et al. 2016; Sandler et al. 2018). ResNet first introduced residual connections, which can help in reducing the problem of accuracy becoming saturated and then degrading rapidly with increasing network depth. DenseNet improves the short-cut mechanism, connects each layer to every other layer in a feed-forward fashion. MobileNet-V2 was designed to reduce network parameters for real-time utilization for portable devices.

Researchers often treat wood classification as a texture classification task. Gray-level co-occurrence matrix (GLCM), local binary pattern (LBP), and gabor filters are popular techniques for the analysis of textures and pattern discrimination (Haralick et al. 1973; Ojala et al. 1996; Olshausen and Field 1996). Paula Filho et al. (2014) compared those techniques combined with a support vector machine to classify 41 Brazilian forest species based on cross section images. Other techniques for wood identification through macroscopic images have also been proposed (e.g., Alfonso et al. 1989; Martins et al. 2013; Ravindran et al. 2018). However, most of the wood identification studies are based on the clean-cut cross section and follow human expert knowledge. This approach may hinder the real industry application where longitudinal sections are commonly found and surfaces are rough (see Sect. Data pre-processing). Recent research in computer vision has shown that CNNs can learn texture instead of shape (Geirhos et al. 2019). Since images of the longitudinal section of boards contain almost all low-frequency texture features, applying CNNs to these images is an obvious choice for species detection. In this work, CNNs were applied to images of longitudinal lumber sections to develop an industrial application for wood species classification.

Materials and methods

The pipeline of a CNN classification task is composed of the following steps: 1) data pre-processing, 2) building of CNN networks, 3) training, 4) testing and evaluation. In the sections below, each step is described in detail.



Fig. 1 Sample images. The area of one pixel corresponds to 0.004 mm²

Table 1 Species list: Board # represents the number of boards we screened, and patch # is the final patch (70 × 70 pixels) count for each species. Alder has the original resolution of 500 × 1000 pixels which is 20 times larger than other boards

Species	Common name	Board #	Patch #
<i>Alnus serrulata</i>	Alder	81	15714
<i>Fraxinus sp.</i>	Ash	200	2478
<i>Tilia americana</i>	Basswood	40	480
<i>Prunus serotina</i>	Cherry	48	576
<i>Acer saccharum</i>	Hard maple	818	9816
<i>Carya ovata</i>	Hickory	13	156
<i>Quercus rubra</i>	Red oak	478	5736
<i>Acer saccharinum</i>	Soft maple	720	8640
<i>Juglans nigra</i>	Walnut	66	792
<i>Quercus sp.</i>	White oak	586	7032
<i>Liriodendron tulipifera</i>	Yellow poplar	108	1296
Total		3158	52716

Data pre-processing

Manually labeled longitudinal images of 11 hardwood species (Fig. 1 and Table 1) were acquired by Microtec Goldeneye 300 Multi-Sensor Quality Scanner™. The lumber used in this study was “rough”, random width, random length, and kiln-dried. These are industry terms that mean that the lumber was unsorted, of varying lengths and widths, moisture content of 6–8 percent, and the surface was not planed, sanded, or otherwise cleaned. Such surface is called rough because it is cut by a sawmill band saw, then air-dried and kiln-dried for several weeks or months. Boards are often dipped in an anti-stain chemical solution prior to air drying to protect against staining and decay. This treatment tends to preserve the natural color of wood somewhat. Additionally, walnut lumber is steamed prior to drying to achieve a uniform, brown color. As boards travel on conveyors throughout the sawmill and then spend time in the yard and kilns, the surface becomes somewhat weathered and possibly marked by the handling and processing equipment. Additionally, drying stickers can often leave marks on the board surface. This is an important distinction from the identification of wood-based on clean or freshly surfaced wood samples. In this study, each board is represented by two images, one on top and one on the bottom board face, and the area of one

pixel corresponds to 0.004 mm². We sampled several image patches (70 pixels × 70 pixels) from each board without overlapping. Subsequently, we applied the up-sampling of all patches by using bi-linear interpolating into 224 × 224, which are commonly used input sizes. In total, we processed 3,158 lumber images, or 52,716 patches, which are listed in Table 1. Hickory is uncommon commercial hardwood species, and its production runs are limited (Settle and Gonso 2020). It was available to us during the data collection process only in a limited volume.

To fully evaluate the performance of CNN, stratified *k* folds cross-validation was applied to the whole data-set. Cross-validation is a common technique used in machine learning (Stone 1974). We applied stratified five folds (20% each) cross-validation without overlapping (Fig. 2). For each experiment, four folds of data (80%) were used during training, as the training set (70%) and validation set (10%), and the rest one-fold of the data (20%) was the test set. Data splitting was performed at the board level. Training set and validation set were used in the training phase. The training set was used to train CNN, while the validation set was used as the indicator for the choice of final model parameters. In the current experiments, the final model weights were selected based on maximizing the accuracy of the validation set. Finally, the reported accuracy is based on the test set.

Architecture

The state-of-the-art CNN architectures were used: ResNet, DenseNet, and MobileNet. These architectures contain several versions, which differ in the total number of layers. In this study, based on the 10-thousand-level data-set size, the relatively shallow version of the above-mentioned CNNs was selected: Resnet-50, DenseNet-121, and MobileNet-V2. Table 2 summaries the selected computing parameters. Resnet-50 has the largest number of parameters (25.55M) and best predicting performance. However, as the trade-off for larger parameter space, Resnet-50 performs slower during the inference phase and may become difficult to train or easy to overfit when the data-set is small. DenseNet-121 and MobileNet-V2 are advanced architectures that reduce parameter numbers (7.98M and 3.50M, respectively) and speed up inference time while retaining as high

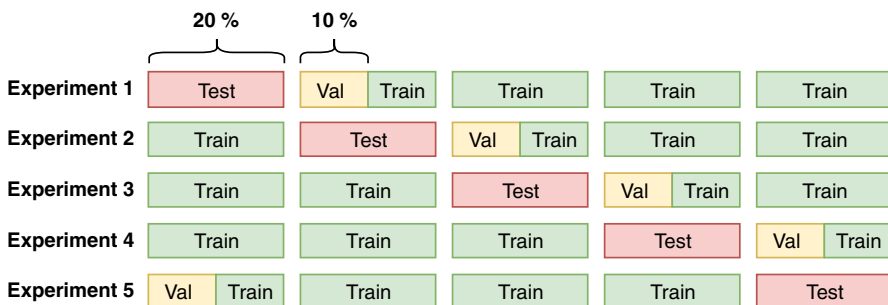


Fig. 2 Visualization of the cross-validation and splitting of data. Test, Val, and Train represent test set, validation set, and train set, respectively. A rectangle is 20 % of the whole data

Table 2 Parameter Numbers, FLOPS and estimated wall times of CNNs. The estimation is based on a 10 GFLOPS device

	Params (M)	FLOPS (G)	Wall time (ms)
ResNet-50	25.55	4.14	414
DenseNet-121	7.98	2.90	290
MoblieNet-V2	3.50	0.33	33

classification accuracy as possible. Table 2 shows the number of parameters and the floating-point operations per second (FLOPS) for each model. FLOPS is a model inference speed quantification and it provides information about the inference time when the device capacity is known. We also show an estimated wall time of each model when processing one image. The estimation is based on a 10 GFLOPS device which is common for CPU. The real inference speed is related to FLOPS and it also depends on the implementation. While DenseNet-121 has smaller FLOPS than ResNet-50, the training and inference time of DenseNet-121 are in the current implementation.

Training

SGD optimizer with a mini-batch size of 64, momentum of 0.9, and Cross-Entropy loss was used for the training of all models. To further validate the effects of the optimizer, we use the same learning rate, and we also use the Adam optimizer to train those models. The learning rate used in Adam optimizer varies from SGD because Adam is a self-adaptive optimizer. Common computer vision data augmentation methods for rotation, flip, and transforming images into gray-scale were used. An identical learning rate schedule was used for all three models. First, we trained all networks with an initial learning rate of 0.045 for 30 epochs with a weight decay of 0.94 for two epochs. Subsequently, we picked the model weights, which performed the best on the validation set, and used the initial learning rate of 0.025 with the same weight decay strategy for ten more epochs. We repeated the second step, but used the initial learning rate of 0.001 for five more epochs. The second and third steps are based on the observation that validation set accuracy tends to fluctuate, indicating that the current learning rate is too large. This training strategy is efficient for data mining competitions with relatively small data-sets and can be considered as a regularization (Goodfellow et al. 2016).

Using a pre-trained model is a transfer learning method, which works well in a small to medium-sized data-set. Common practical transfer learning approaches for classification tasks are based on a two-step method - first, train the last fully connected layer and freeze the remaining layers for several epochs, and then, fine-tune the entire network. This two-step method can stabilize the entire training process. However, based on our preliminary tests, this two-step method does not perform better than a single-step transfer learning, which trains the entire network directly. We further discuss this in the Ablation study section.

Testing and evaluation

Ensemble learning is useful to improve accuracy during the testing phase. We used majority voting and models ensemble to enhance the robustness and performance of the results. The majority of voting is suitable for our purposes since patch images are sampled from boards. Depending on different wood species, the number of images per board is either 12 or 14, except for alder (194). The majority voting applied to board level classification leads to incremental results. The model ensemble is the summary of all probability outputs per class of all the above models as the ensemble output. We used a simple probability ensemble with equal weight for all three models in this research.

Results and discussions

This system has been implemented on a desktop computer equipped with Intel® Core™ i7-8700K CPU @ 3.70GHz ×12 , with 32 GB of memory, and with NVIDIA® GeForce® RTX 1080 Ti GPU. All the implementations of models are based on PyTorch 1.4.

Table 3 shows the overall accuracy and the macro F1 of the predictions of our models. Even though our data-set is not very balanced, the macro F1 is still aligned with accuracy in our cases. So in the following, focus will be on analyzing accuracy for simplicity. For single model, ResNet-50 performs best in both patch and lumber identification (0.9519 and 0.9815, respectively), followed by DenseNet-121 (0.9384 and 0.9755) and MobileNet-V2 (0.9352 and 0.9712). The performance order of the three model architectures is also in line with models trained and evaluated by the ImageNet data-set. For ensemble models, as expected, the top-1 accuracy slightly increases compared to any single model in patch identification. However, for lumber identification, ensemble models do not exceed the performance of ResNet-50. This fact generally indicates that the performance of all single models is highly correlated.

Table 3 Model performance. The value is represented as mean ± variance for 5 models

Data level	Model	Accuracy	Macro F1
Patch	ResNet-50	0.9519 ± 0.0065	0.8893 ± 0.0231
	DenseNet-121	0.9384 ± 0.0078	0.8634 ± 0.0323
	MobileNet-V2	0.9352 ± 0.0185	0.8507 ± 0.0363
	Average ensemble	0.9560 ± 0.0075	0.8944 ± 0.0330
Board	ResNet-50	0.9815 ± 0.0079	0.9558 ± 0.0237
	DenseNet-121	0.9755 ± 0.0088	0.9408 ± 0.0401
	MobileNet-V2	0.9712 ± 0.0095	0.9076 ± 0.0446
	Average ensemble	0.9772 ± 0.0087	0.9424 ± 0.0420

Best values are indicated in bold

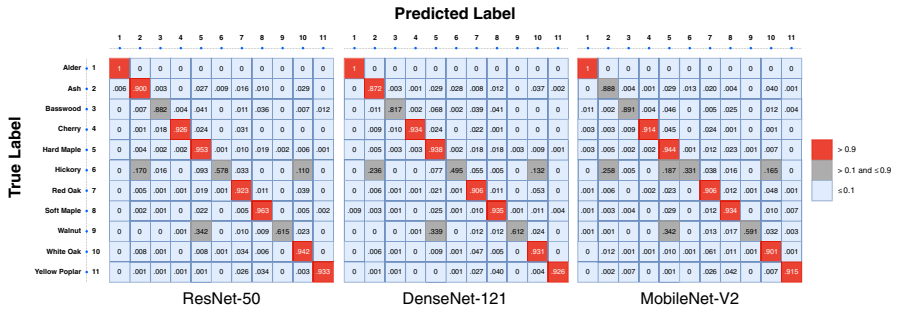


Fig. 3 Patch level confusion matrix for three models. The x-axis represents the predicted label of models, and the y-axis represents the true label of the patch. Numbers and their corresponding species names are listed on the y-axis. The numbers represent the proportions of the predicted label for one species and should sum up to one

Table 4 Precision and Recall scores for each species based on patch level prediction and ResNet-50 model

Species	Common name	Precision	Recall
<i>Alnus serrulata</i>	Alder	0.9999	0.9940
<i>Fraxinus sp.</i>	Ash	0.8719	0.9071
<i>Tilia americana</i>	Basswood	0.8179	0.8529
<i>Prunus serotina</i>	Cherry	0.9330	0.9194
<i>Acer saccharum</i>	Hard maple	0.9392	0.9210
<i>Carya ovata</i>	Hickory	0.4945	0.4286
<i>Quercus rubra</i>	Red oak	0.9056	0.8793
<i>Acer saccharinum</i>	Soft maple	0.9341	0.9553
<i>Juglans nigra</i>	Walnut	0.6126	0.9264
<i>Quercus sp.</i>	White oak	0.9299	0.9127
<i>Liriodendron tulipifera</i>	Yellow poplar	0.9253	0.9576

The patch level confusion matrix for all single models is shown in Fig. 3. For model comparison, similar to the above-discussed overall accuracy, ResNet-50 performs best in all species classification. Hickory is the most challenging to identify. In Table 4, the precision and recall of hickory are far less than other species, which also proves the difficulty. One reason is that the training sample is not large: only 156 patches for the whole data-set. Moreover, hickory is also similar to ash, which is in line with traditional wood identification. Ash and hickory are ring porous species with visible rays, visible parenchyma cells and relative dark color, leading to similar patterns in longitudinal section. Alder becomes easiest to identify in patch identification. We need to point out that the high accuracy of the alder patch might not transform to the real-world application because the image resolution and shape of alder are different from other species in the collected data-set.

When diving into the board-level confusion matrix (see Fig. 4), majority voting plays a critical role in increasing the accuracy. All three models behave similarly,

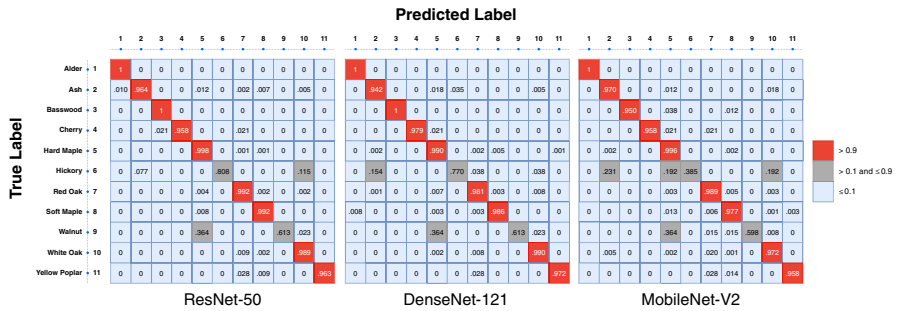


Fig. 4 Board level confusion matrix for three models. Here x-axis is the predicted label of models, while the y-axis is the true label of the board. Numbers and their corresponding species names are listed on the y-axis. The numbers in each line represent the proportions of the predicted label for one species and should sum up to one

except predicting hickory in DenseNet-121. One Densenet-121 model out of five failed to identify hickory since the hickory set is small.

The present method has several limitations. First, the data-set is not balanced. There are 11 species with a total of 3,158 boards. However, some species, for example, hickory, have less than 0.5% (13/3158) of total boards. This non-balanced issue may affect the results when the trained models are transformed into a real-world application when the unknown species distributions do not parallel those of our data-set. Data sampling and weight method might relieve this problem, but will not help when the imbalance rate is significant. In the future, it is planned to collect more data from overcoming this issue. Second, some lumber samples exhibited dark stains (see Fig. 1) that are not part of the natural anatomy of wood. Instead, they are very common lumber processing marks. In this case, we consider it as the bias in our data-set that might potentially slightly help to increase the final accuracy of CNNs, since these stains appear most frequently in Soft and Hard Maple lumber. The present data does not have labels from the tree level, which may lead to an overestimation of the performance. US hardwood industry is fragmented. While there are few large companies, most are small to medium-sized. The nature of the wood industry is such that processing of rough, kiln-dried lumber in factories that utilize a scanner in their process is far removed from the tree harvesting and board milling operations. It is not uncommon for a sawmill to have several hundred small local log suppliers. Each board goes through processes of sawmilling, green grading, sorting by species, length, width, thickness, and grade. When a sufficient quantity is accumulated in each subgroup, the green lumber is sold or air-dried at the mill. Then, it is re-graded and sorted, kiln-dried, graded, and sorted again. When sufficient quantity is accumulated in each sub-group, it is sold and possibly goes through other merchandising steps at concentration yards, distribution yards, and international trade. A secondary wood products manufacturer typically has dozens of lumber suppliers. While the likelihood that any two boards in a package of lumber at a secondary wood processing facility came from the same region is moderately high, the likelihood that

Table 5 Ablation study. The value is represented as mean \pm variance for 5 models. Here s is the input size to the model

Experiment	Model	Accuracy	Accuracy
		$s = 224$	$s = 70$
Baseline	ResNet-50	0.9519 \pm 0.0065	0.9192 \pm 0.0197
	DenseNet-121	0.9384 \pm 0.0078	0.8846 \pm 0.0217
	MobileNet-V2	0.9352 \pm 0.0185	0.8942 \pm 0.0231
Using Adam as optimizer	ResNet-50	0.9344 \pm 0.0080	0.9135 \pm 0.0064
	DenseNet-121	0.9483 \pm 0.0025	0.9173 \pm 0.0062
	MobileNet-V2	0.9391 \pm 0.0049	0.9093 \pm 0.0060
Removing gray-scale augmentation	ResNet-50	0.9585 \pm 0.0129	0.9186 \pm 0.0139
	DenseNet-121	0.9467 \pm 0.0093	0.9033 \pm 0.0119
	MobileNet-V2	0.9561 \pm 0.0069	0.8746 \pm 0.0328
Using two step transfer learning	ResNet-50	0.9264 \pm 0.0153	0.8734 \pm 0.0169
	DenseNet-121	0.9338 \pm 0.0085	0.8663 \pm 0.0107
	MobileNet-V2	0.9227 \pm 0.0137	0.8273 \pm 0.0384

Table 6 Model accuracy after removing maple data. The value is represented as the mean \pm and the variance for five models. Here s is the input size to the model

Model	Accuracy	Accuracy
	$s = 224$	$s = 70$
ResNet-50	0.9550 \pm 0.0069	0.9169 \pm 0.0384
DenseNet-121	0.9433 \pm 0.0039	0.8931 \pm 0.0267
MobileNet-V2	0.9366 \pm 0.0400	0.8875 \pm 0.0277

any two boards came from the same tree is extremely low. Such point-of-origin information is not kept or available for industrial lumber. Due to these facts, we consider our lumber sample for each species to have sufficient between-trees variation within the US Midwest hardwood region. While there may be slight appearance variation in woods from different regions, their anatomical features do not differ significantly within the species. Therefore, the results of this study should transfer to other regions of the hardwood industry.

Ablation study

An ablation study is presented that reports patch accuracy, where the difference is measurable. Tables 5 and 6 list the experiments. The baseline refers to the pipeline described in Materials and methods section.

The input size of the image is critical for model performance. Table 5 shows that when the input size of images is replaced from 70×70 to 224×224 , where those images are almost identical since the later images are just re-scale from the

former ones, the model accuracy increases approximately 2-3 percentages. The possible explanation is that for large input, zero padding effects decrease, thus improving accuracy.

SGD and ADAM (Kingma and Ba 2015) are commonly used to optimize the model. In most conditions, SGD is slower, but theoretically guarantees to converge, while ADAM is slightly faster but may not guarantee the convergence. Table 5 shows that, in the present scenario, ADAM performs similar to SGD, but ADAM is more suitable for DenseNet-121 than ResNet-50 and MobileNet-V2.

The initial intention was to use gray-scale augmentation to train a more robust model because we considered grain to be a more robust feature than color. By removing gray-scale augmentation (see Table 5), a slightly more accurate model was obtained.

The effects of the two-step transfer learning method were also tested: first, train the last fully connected layer and freeze the remaining layers for several epochs, and then fine-tune the entire network. The parameter of the feature extractor was fixed for the first six epochs. Table 5 shows that two-step methods performed slightly worse than training the model directly. This phenomenon typically happened when the input domain was very different from the pre-trained data to new data.

Table 6 shows the model performance after removing maple species.

Conclusion

In this study, the potential use of CNNs for hardwood lumber identification based on tangential plane images was investigated. We achieved over 95% successful classification rate for a single model and 98% by applying the model ensemble. The selected CNNs can identify lumber through the tangential plane correctly. In the future, we will focus on analyzing the feature importance of our data by removing specific features and comparing the decrements of performance for different species.

Acknowledgements This research was supported by the Foundation for Food and Agriculture Research Grant ID: 602757 to Benes and McIntire Stennis grant accession no. 1012928 to Gazo from the USDA National Institute of Food and Agriculture. The content of this publication is solely the responsibility of the authors and does not necessarily represent the official views of the respective funding agencies.

Compliance with ethical standards

Conflicts of interest The authors declare that they have no conflict of interest.

References

- Alfonso V, Baas P, Carlquist S, Chimelo J, Coradin V, Détienne P, Gasson P, Grosser D, Ilic J, Kuroda K, Miller R, Ogata K, Richter H, Welle B, Wheeler E (1989) Iawa list of microscopic features for hardwood identification: with an appendix on non-anatomical information. *IAWA J* 10:221–358. <https://doi.org/10.1163/22941932-90000496>
- Gazo R, Wells L, Krs V, Benes B (2018) Validation of automated hardwood lumber grading system. *Comput Electron Agric* 155:496–500. <https://doi.org/10.1016/j.compag.2018.06.041>

- Geirhos R, Rubisch P, Michaelis C, Bethge M, Wichmann FA, Brendel W (2019) ImageNet-trained CNNs are biased towards texture; increasing shape bias improves accuracy and robustness. In: Proc. 6th Int. Conf. Learn. Represent. <https://openreview.net/forum?id=Bygh9j09KX>
- Goodfellow I, Bengio Y, Courville A (2016) Deep learning. MIT press, Cambridge
- Haralick RM, Shanmugam K, Dinstein IH (1973) Textural features for image classification. *IEEE Trans Syst Man Cybern Syst SMC* 3(6):610–621. <https://doi.org/10.1109/TSMC.1973.4309314>
- He K, Zhang X, Ren S, Sun J (2016) Deep residual learning for image recognition. In: Proc. IEEE Comput. Soc. Conf. Comput. Vis. Pattern Recognit., pp 770–778. <https://doi.org/10.1109/CVPR.2016.90>
- Huang G, Liu Z, Van Der Maaten L, Weinberger KQ (2017) Densely connected convolutional networks. In: Proc. IEEE Comput. Soc. Conf. Comput. Vis. Pattern Recognit., pp 4700–4708 <https://doi.org/10.1109/CVPR.2017.243>
- Ioffe S, Szegedy C (2015) Batch normalization: Accelerating deep network training by reducing internal covariate shift. In: Proc. 32nd Int. Conf. Mach. Learn., pp 448–456
- Kingma DP, Ba J (2015) Adam: A method for stochastic optimization. In: Proc. 3rd Int. Conf. Learn. Represent
- Lecun Y, Bottou L, Bengio Y, Haffner P (1998) Gradient-based learning applied to document recognition. *Proc IEEE* 86(11):2278–2324. <https://doi.org/10.1109/5.726791>
- Martins J, Oliveira L, Nisgoski S, Sabourin R (2013) A database for automatic classification of forest species. *Mach Vis Appl* 24(3):567–578. <https://doi.org/10.1007/s00138-012-0417-5>
- Ojala T, Pietikäinen M, Harwood D (1996) A comparative study of texture measures with classification based on featured distributions. *Pattern Recognit* 29(1):51–59. [https://doi.org/10.1016/0031-3203\(95\)00067-4](https://doi.org/10.1016/0031-3203(95)00067-4)
- Olshausen BA, Field DJ (1996) Emergence of simple-cell receptive field properties by learning a sparse code for natural images. *Nature* 381(6583):607–609. <https://doi.org/10.1038/381607a0>
- Paula Filho PL, Oliveira LS, Nisgoski S, Britto AS (2014) Forest species recognition using macroscopic images. *Mach Vis Appl* 25(4):1019–1031. <https://doi.org/10.1007/s00138-014-0592-7>
- Ravindran P, Costa A, Soares R, Wiedenhoeft AC (2018) Classification of cites-listed and other neotropical meliaceae wood images using convolutional neural networks. *Plant methods* 14(1):25
- Sandler M, Howard A, Zhu M, Zhmoginov A, Chen LC (2018) Mobilenetv2: Inverted residuals and linear bottlenecks. In: Proc. IEEE Comput. Soc. Conf. Comput. Vis. Pattern Recognit., pp 4510–4520. <https://doi.org/10.1109/CVPR.2018.00474>
- Settle J, Gonso C (2020) 2020 Indiana forest products price report and trend analysis. Tech. rep, Indiana Department of Natural Resources. <https://www.in.gov/dnr/forestry/files/fo-spring-price-report-2020.pdf>
- Srivastava N, Hinton G, Krizhevsky A, Sutskever I, Salakhutdinov R (2014) Dropout: a simple way to prevent neural networks from overfitting. *J Mach Learn Technol* 15(1):1929–1958
- Stone M (1974) Cross-validators choice and assessment of statistical predictions. *J R Stat Soc Series B Stat Methodol* 36(2):111–133
- Wells L, Gazo R, Del Re R, Krs V, Benes B (2018) Defect detection performance of automated hardwood lumber grading system. *Comput Electron Agric* 155:487–495. <https://doi.org/10.1016/j.compag.2018.09.025>

Publisher's Note Springer Nature remains neutral with regard to jurisdictional claims in published maps and institutional affiliations.